BIBLIOGRAPHIC INFORMATION SYSTEM

Journal Full Title: Journal of Biomedical Research & Environmental Sciences

Journal NLM Abbreviation: J Biomed Res Environ Sci

Journal Website Link: https://www.jelsciences.com

Journal ISSN: 2766-2276

Category: Multidisciplinary

Subject Areas: Medicine Group, Biology Group, General, Environmental Sciences

Topics Summation: 128

Issue Regularity: Monthly

Review Process type: Double Blind

Time to Publication: 7-14 Days

Indexing catalog: Visit here

Publication fee catalog: Visit here

DOI: 10.37871 (CrossRef)

Plagiarism detection software: iThenticate

Managing entity: USA

Language: English

Research work collecting capability: Worldwide

Organized by: SciRes Literature LLC

Manuscript should be submitted in Word Document (.doc or .docx) through

Online Submission

form or can be mailed to support@jelsciences.com

Vision: Journal of Biomedical Research & Environmental Sciences main aim is to enhance the importance of science and technology to the scientific community and also to provide an equal opportunity to seek and share ideas to all our researchers and scientists without any barriers to develop their career and helping in their development of discovering the world.

JOURNAL OF BIOMEDICAL RESEARCH & ENVIRONMENTAL SCIENCES
issn: 2766-2276
SUBJECT AREA(S): BIOINFORMATICS | BIOLOGY
DOI: 10.37871

RESEARCH ARTICLE

Bioinformatic Analysis of the Association Between Myocardial Disease and Diesel Particulate Matter

Kyoung Jin Nho* and Jae Hoon Shin

Institute of Occupation and Environment, COMWEL, 478, Munemi-ro, Bupyeong-gu, Incheon, 21417, Republic of Korea

ABSTRACT

The etiological connection between Diesel Particulate Matter (DPM) and heart failure is unclear, despite the fact that multiple experimental studies have found a strong correlation between DPM and heart failure. We investigated the correlation between DPM and myocardial infarction using biological big data. Distinct gene expression profiles related to DPM and myocardial infarction were obtained from open-access genome databases, and a network analysis software was used to investigate their interaction. We investigated the detrimental effects of DPM on cardiac cells to understand the association between them. The putative signaling networks of 33 genes with differential expression were identified and studied. In addition to increasing the prediction accuracy, our study used experimental validation and literature-based analysis to enhance the knowledge of the mechanisms underlying DPM-related cardiac disease.

Abbreviations

DPM: Diesel Particulate Matter; GEO: Gene Expression Omnibus; DEGs: Differentially Expressed Genes; GO: Gene Ontology; KEGG: Kyoto Encyclopedia of Genes and Genomes; DAVID: Database for Annotation, Visualization, and Integrated Discovery; PPI: Protein-Protein Interaction

Introduction

Cardiac hypertrophy and ischemic injury (myocardial infarction) are major risk factors for heart failure and sudden death [1-3]. Pathophysiological stress in the heart causes physiological changes accompanied by transcriptional and epigenetic changes. This is characterized by increased cell size and extracellular matrix accumulation due to a variety of cardiovascular disorders, including pressure overload, heart valve dysfunction, and congestive heart failure [4-6]. Myocardial infarction continues to be one of the major causes of death worldwide despite significant improvements in therapy and prevention measures. Therefore, understanding the mechanisms underlying the development of cardiac hypertrophy, and myocardial infarction is essential for the prevention, and treatment of these diseases.

Diesel Particulate Matter (DPM) is a known carcinogenic factor and major air pollutant in cities [7,8]. The biological effect of particulate matter,

***Corresponding author(s)**

Kyoung Jin Nho, Institute of Occupation and Environment, COMWEL, 478, Munemi-ro, Bupyeong-gu, Incheon, 21417, Republic of Korea

Email: nkj1130@comwel.or.kr

DOI: 10.37871/jbres1714

Submitted: 24 March 2023

Accepted: 03 April 2023

Published: 04 April 2023

Keywords

- Diesel particulate matter
- Myocardial infarction
- H9C2 cells
- Gene expression omnibus

BIOLOGY GROUP

BIOINFORMATICS | BIOLOGY

VOLUME: 4 ISSUE: 4 - APRIL, 2023

How to cite this article: Nho KJ, Shin JH. Bioinformatic Analysis of the Association Between Myocardial Disease and Diesel Particulate Matter. 2023 Apr 04; 4(4): 590-599. doi: 10.37871/jbres1714, Article ID: JBRES1714, Available at: https://www.jelsciences.com/articles/jbres1714.pdf

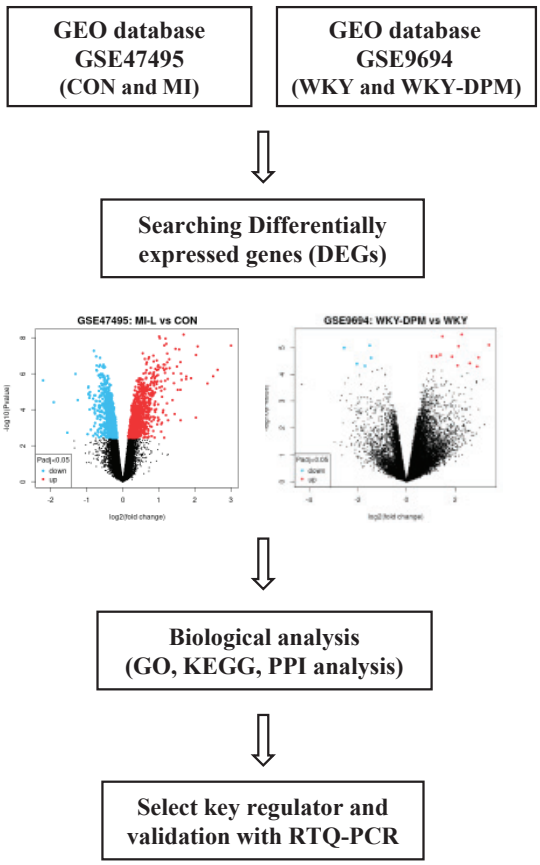

Figure 1 Study design scheme.

such as DPM, is strongly related to its diameter. DPM majorly consisting of respirable particles less than 2.5 μm is classified as PM2.5. Exposure to DPM is a potential health hazard in large cities, where traffic is heavy resulting in air pollution and environments where diesel engines operate [9]. DPM is affected by fuel source, engine type, and operating conditions. Owing to its small particle size, DPM remains in the atmosphere for a long duration, adsorbing harmful substances such as various trace metals, Polycyclic Aromatic Hydrocarbons (PAHs), and nitroarenes, showing various chemical variabilities [10]. DPM enters cells, attaches to blood vessels, causes respiratory diseases, and move to other tissues through the blood, causing cardiovascular and lung function aggravation over long-term exposure, eventually leading to death [11]. Many studies have been reported on the effects of DPM on heart disease. According to previous studies, the correlation between increase in myocardial disease incidences and mortality, caused by exposure to DPM in the air has been clearly identified [12-14], but its biological pathogenesis remains unclear. Most previous studies have focused on the mechanism by which DPM exposure increases Reactive Oxygen Species (ROS) formation and the resulting inflammatory mediators expression [15,16]. However, studies on gene expression patterns are limited. Therefore, this study screened DPM and myocardial infarction data expression profiles from the Gene Expression Omnibus (GEO) database. Based on the analysis results, we selected genes involved in the myocardial disease network according to DPM treatment. Furthermore, verification experiments such as quantitative real-time-polymerase chain reaction (qRT-PCR) should be conducted and the genes involved in the induction and exacerbation of myocardial disease by DPM need to be identified.

Materials and Methods

Materials

Labware including multi-well plates, serological pipettes, and spreaders, were bought from BD Falcon (Franklin Lakes, NJ, USA) and Corning Incorporated (Corning, NY, USA). Paraformaldehyde (4%) and Triton X-100 (0.1%) were bought from Sigma-Aldrich (St. Louis, MO, USA).

Table 1: Details for GSE47495 and GSE9694 data series.

Accession No.	Platform	Sample	Organism	Group
GSE47495	GPL6247	Left ventricular tissue	Rattus norvegicus	CON = sham-operated rat (*n* = 6) MI = myocardial infarction (*n* = 5)
GSE9694	GPL341	Heart	Rattus norvegicus	WKY = wistar kyoto rat air exposure (*n* = 4) WKY-DPM = wistar kyoto rat diesel exposure (*n* = 4)

Preparation of DPM

Standard Reference Material 1650b (SRM1650b) was purchased from the National Institute of Standards and Technology (NIST). Refer to NIST (1650b.pdf (nist.gov)) for SRM1650b certificate of analysis. SRM1650b was suspended in Phosphate-Buffered Saline (PBS) at 10 mg/mL stock concentration.

Searching data and identification of differentially expressed genes

Expression profiles of DPM and myocardial infarction were acquired from the Gene Expression Omnibus (GEO) database; two independent data series, GSE47495 and GSE9694, were used in our study. The following keywords were used to screen gene expression datasets: diesel particulate matter, gene expression profiles by array, Rattus norvegicus, cardiac hypertrophy, myocardial infarction, and heart failure. The details of the two data series are listed in table 1, and figure 1 displays the study design plan. GEO2R is an online tool that allows comparisons between two groups of samples to analyze the GEO database using the limma R package. We analyzed the DEGs as differentially expressed genes in GSE47495 under the condition of adj. $p < 0.05$ and $\log(FC) \geq 1.5$. In addition, GSE9694 was analyzed with an adj. p -value < 0.05, and $\log(FC) > 1$.

Functional enrichment analysis

The molecular correlation between myocardial infarction and DPM was examined using Gene Ontology (GO) and Kyoto Encyclopedia of Genes and Genomes (KEGG) pathway analyses using the Database for Annotation, Visualization, and Integrated Discovery (DAVID) and ShinyGO 0.77 online tools. A Shiny application called ShinyGO is built on a number of R/Bioconductor programs, as well as a sizable annotation and pathway database compiled from multiple sources. The functional categories of Biological Process (BP), Cell Components (CC), and Molecular Functions (MF) were included in the GO enrichment. By measuring and rating the gene count simultaneously, meaningful GO biological processes and pathway enrichment analyses were selected, with statistical significance set at $p < 0.05$. Data analysis and visualization were done using the ShinyGo enrichment tool.

PPI network

The online database Search Tool for the Retrieval of Interacting Genes/Proteins was used to analyze the Protein-Protein Interaction (PPI) network between myocardial infarction and DPM (STRING: functional protein association networks (string-db.org)).

Cell culture and treatments

H9C2 cells were purchased from the American Type Culture Collection (ATCC) (Manassas, VA, USA) and propagated according to the instructions provided. Dulbecco's Modified Eagle's medium (DMEM) was used to sustain cells on a regular basis. It contains 10% fetal bovine serum from ATCC and 1% penicillin-streptomycin (Gibco BRL, Gaithersburg, MD, USA).

Cells were incubated at 37°C and 5% carbon dioxide. Before treatment, the stock solution was sonicated for 1h in an ultrasonic bath to adequately disperse particulate matter. The stock solution was diluted with DMEM for treatment. After treatment, each well was washed twice with PBS to reduce the effect of the remaining particles.

Immunofluorescence staining

Cell surface measurements followed previous studies [17]. Briefly, H9C2 cells cultured on the coverglass were washed with PBS and then fixed with 4% paraformaldehyde for 10 min. Again, washed twice with PBS, and permeabilized with 0.1% Triton X-100 in PBS. After blocking with 1% BSA in PBS for 1h at room temperature, cells were incubated with an anti-α-actinin antibody, conjugated to Alexa Fluor 488. 4',6-diamidino-2-phenylindole (DAPI) was used to stain the nuclei (Molecular Probes, Eugene, OR, USA). After washing, the slides were mounted using a fluorescent mounting medium. Axio Imager M2 microscope from Carl Zeiss (Oberkochen, Germany), was used to examine the prepared cells, and ZEISS ZEN 3.7 software was used for analysis (Carl Zeiss).

RNA extraction and quantitative real-time PCR (qRT-PCR)

H9C2 cells treated with DPM were prepared, and total RNA was extracted using PureLink RNA mini kit (Invitrogen, USA). For cDNA synthesis, High-Capacity RNA-to-cDNA Kit was used (Applied Biosystems, Waltham, MA, USA). The primer used for qRT-PCR shown in Table 2. QuantStudio 3 Real-Time PCR System and SYBR green dye from Applied Biosystems to analyze and quantify the expression levels of mRNA. The mRNA expression was normalized to 18S rRNA, and the comparative Ct (ΔΔCt) method was used for the expression level. All reactions were performed in triplicates.

Statistical analysis

All experimental results were expressed using mean ± standard error of the mean (SEM). For statistical analysis, an unpaired Student's t test or one-way ANOVA method was used. Triplicates of each experiment were conducted. Compared to the control group, $P < 0.05$ was determined to be statistically significant.

Results and Discussion

Identification of DEGs

Microarray results of the GSE47495 and GSE9694 DEGs were screened using GEO2R. The details of the two data series are listed in table 1. GSE47495 included five left ventricular tissue samples from rats undergoing Myocardial Infarction (MI) surgery and six left ventricular tissue samples from rats undergoing a sham operation (CON). First, 1,649 DEGs were obtained from the GSE47495 data series (adj. $p < 0.05$, CON vs. MI), including 844 up-regulated and 805 down-regulated genes. Then, the top 18 up-regulated DEGs from the GSE47495 data series were acquired with the criteria of log(FC) ≥ 1.5 (Figure 2A and table 3). In addition, the GSE9694 data series obtained included four Wistar Kyoto (WKY) rats exposed to air or the whole body to diesel emission particles for 4 weeks (WKY-DPM). Fifteen DEGs were acquired from the GSE9694 dataset (WKY vs. WKY-DPM), including 11 up-regulated (log(FC) > 1) and four down-regulated (log(FC) < -1.5) with an adj. $p < 0.05$ (Figure 2B and Table 4). Then, we conducted a hierarchical clustering analysis to show DEGs as a heatmap using a SRplot (Figure 2).

Function enrichment analysis and PPI network

To determine the function of the target genes, we conducted GO and KEGG analyses of the interacting 33 DEGs from GSE47495 and GSE9694 using DAVID and ShinyGO 0.77 online tools. Three functional categories: Biological Process (BP), Cell Components (CC), and Molecular Functions (MF) were created from the results of the GO enrichment study. Following DEG analysis, significantly enhanced BP is displayed in a dot plot, clustering tree, and graphical network (Figure 3). The BP results indicated that DEGs were mainly enriched in developmental growth involved in morphogenesis, axis elongation, developmental growth, and negative regulation of Mitogen-Activated Protein Kinase (MAPK) activity (Figures 3A&B). BP with a large number of shared genes is grouped. The enriched terms were arranged into a network with edges connecting overlapping gene sets (Figure 3C). Furthermore, the extracellular region, external encapsulating structure, collagen-containing extracellular matrix, and extracellular matrix were enriched in the CC category (Figure 4A). The most enriched MFs were G protein-coupled receptor binding, glycosaminoglycan binding, inorganic cation transmembrane transporter activity, active ion transmembrane transporter activity, and sulfur compound binding (Figure 4B).

Table 2: Primer lists for qRT-PCR analysis.

Genes	Forward	Reverse	Accession number
Sfrp1	CTGCCACCAGCTGGACAAC	ACCTTGCGCCCCATGAT	NM_001276712.2
Sfrp2	TGTCCGATAGGGACCTGAAGA	GGTGCACTGCAGGCTGTCT	NM_001100700.1
Fzd2	GGATCTGGTCCGGCAAGAC	GTTGGTGAGACGCGTGTAGAAC	NM_172035.2
Atp2a2	TTGGGTTTCCTGAAGCTTTGA	ACCATCCGTCACCAGATTGAC	NM_001110139.2
Atp1a3	CTGTCCTCGGGTTCCGTAAA	GGGAATCTCGGCCACTTTCT	NM_012506.1
Nppa	ACCTGCTAGACCACCTAGAGG	GCTGTTATCTTCCGTACCGG	NM_012612.2
Nppb	CAGCTGCCTGGCCCATCACT	ACCTCCCAGCGGCGACAGAT	NM_031545.1
18S	AAGTTTCAGCACATCCTGCGAGTA	TTGGTGAGGTCAATGTCTGCTTTC	NM_213557.1

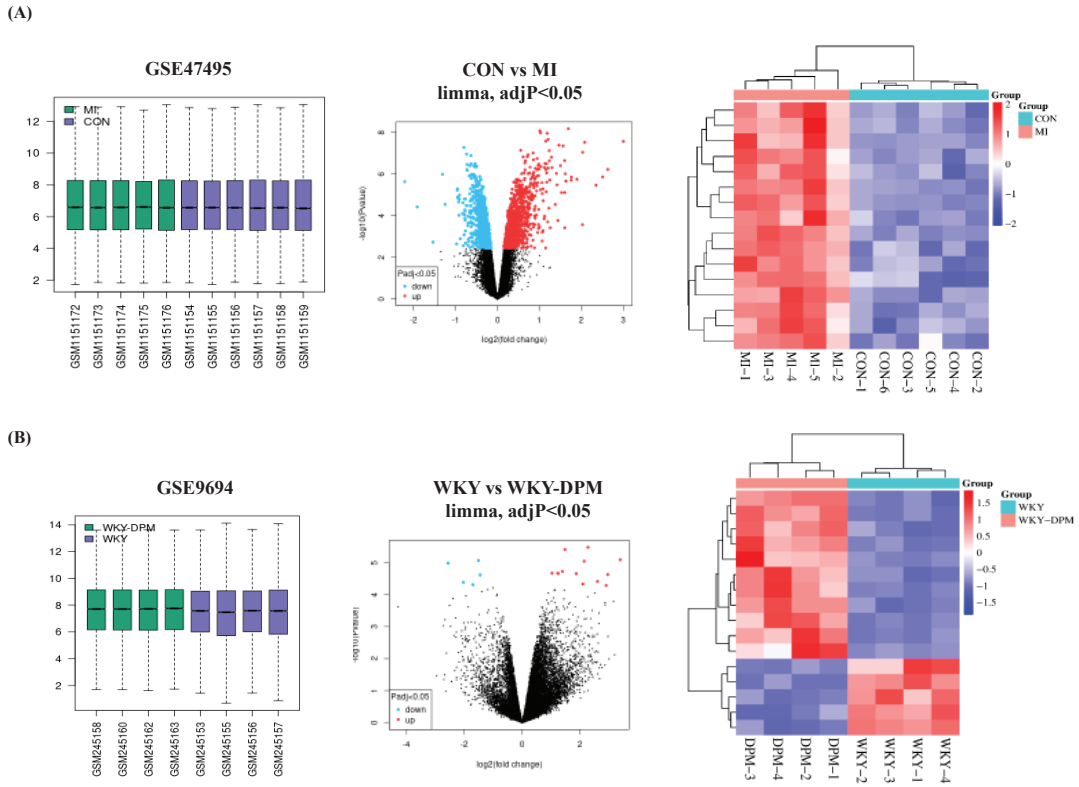

Figure 2 Identification of DEGs. (A) GSE47495: Box plot showing levels of gene probe expression. DEGs between the CON and MI groups on the volcano plot. Upregulated DEGs are represented by the red dot, while downregulated DEGs are represented by the blue dot. Selected DEG expression heatmap. (B) GSE9694: Box plot showing the levels of gene probe expression. DEGs between the WKY and WKY-DPM groups are plotted on volcano. Selected DEG expression heatmap.

Table 3: Top 18 up-regulated DEGs form analysis of the GSE47495 data series.

ID	adj.*p*-Val	*p*-Value	logFC	Gene symbol	Gene title
10815369	0.000111	2.73E-08	3	Postn	periostin
10719728	0.000533	1.39E-06	2.5	Atp1a3	ATPase Na+/K+ transporting subunit alpha 3
10750505	0.000802	3.49E-06	2.35	Pcp4	Purkinje cell protein 4
10706059	0.000111	3.04E-08	2.07	Sbsn	suprabasin
10720829	0.00019	9.10E-08	2.03	Hamp	hepcidin antimicrobial peptide
10940654	0.009324	2.76E-04	2.03	Spp1	secreted phosphoprotein 1
10873899	0.000594	1.79E-06	1.89	Nppa	natriuretic peptide A
10792344	0.000533	1.42E-06	1.76	Sfrp1	secreted frizzled-related protein 1
10816144	0.000605	1.99E-06	1.75	Sfrp2	secreted frizzled-related protein 2
10764069	8.13E-05	6.70E-09	1.69	Chi3l1	chitinase 3 like 1
10717233	0.000644	2.20E-06	1.63	Ctgf	connective tissue growth factor
10842043	0.000466	9.89E-07	1.61	Wisp2	WNT1 inducible signaling pathway protein 2
10927361	0.000262	2.27E-07	1.6	Ankrd23	ankyrin repeat domain 23
10935041	0.001186	7.82E-06	1.6	Tceal7	transcription elongation factor A like 7
10917183	0.011489	3.88E-04	1.6	Ncam1	neural cell adhesion molecule 1
10928761	0.000131	4.48E-08	1.56	Fn1	fibronectin 1
10918869	0.001186	7.88E-06	1.52	Col12a1	collagen type XII alpha 1 chain
10917883	0.000321	4.01E-07	1.5	Loxl1	lysyl oxidase-like 1

adj.*p*-value < 0.05, log(FC) ≥ 1.5.

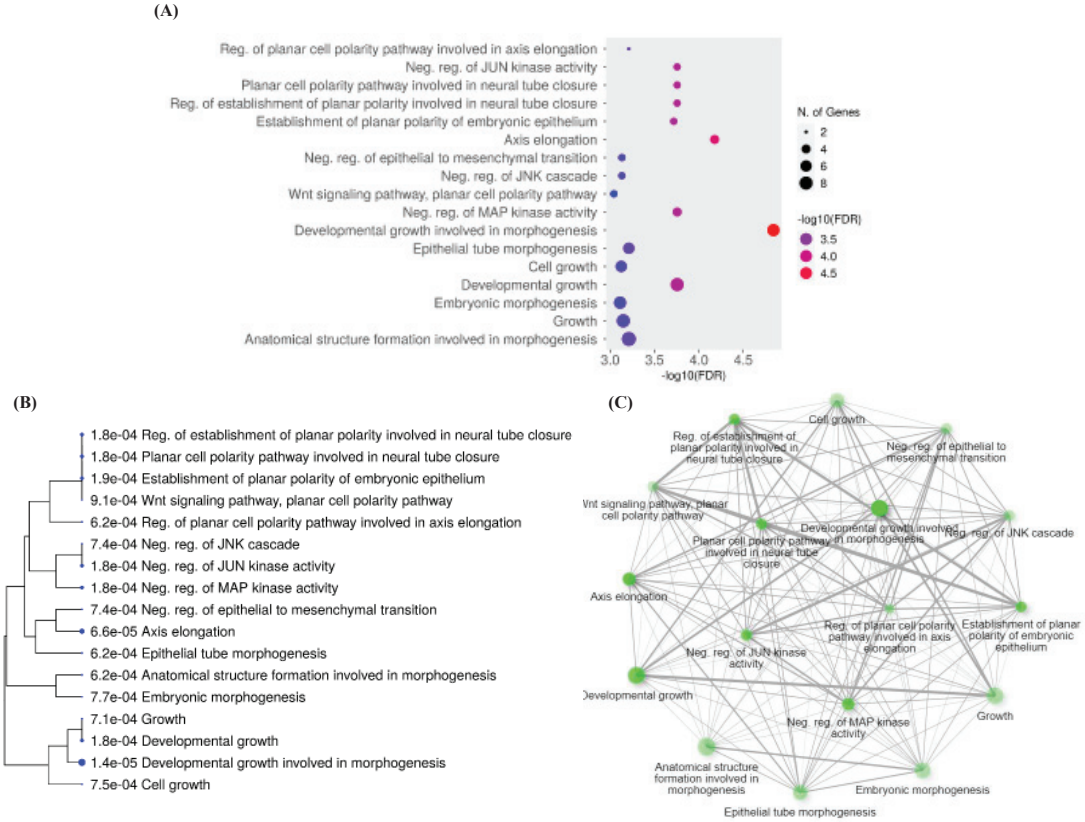

Figure 3 Enriched biological processes in 33 DEGs. (A) The dot plot, (B) clustering tree, and (C) potential biological networks involvement. Following DEG analysis, significantly enhanced BP is displayed in an interactive hierarchical clustering tree. BP is grouped together with several shred genes. Significant p-values are shown by larger dots. After gene expression data analysis, similar enriched biological processes are revealed. FDR p-value cutoff = 0.05 and Edge cutoff = 0.2.

Table 4: Top 15 DEGs from analysis of the GSE9694 data series.

ID	adj.*p*-Val	*p*-Value	logFC	Gene.symbol	Gene.title
1368609_at	0.0294	0.00002337	2.96	Slc10a1	solute carrier family 10 member 1
1389706_at	0.0453	0.00005118	2.90	Dclk1	doublecortin-like kinase 1
1373931_at	0.027	0.00000326	2.28	Pianp	PILR alpha associated neural protein
1369091_at	0.027	0.00000887	2.14	Chrnb1	cholinergic receptor nicotinic beta 1 subunit
1386514_at	0.0453	0.00004622	2.10	Hapln4	hyaluronan and proteoglycan link protein 4
1375539_at	0.0294	0.00002184	1.87	Tbr1	T-box, brain, 1
1388093_at	0.027	0.00000382	1.48	Tas2r126	taste receptor, type 2, member 126
1374587_at	0.0294	0.0000185	1.39	Tmtc3	transmembrane and tetratricopeptide repeat containing 3
1374864_at	0.0294	0.00002153	1.25	Spry2	sprouty RTK signaling antagonist 2
1375164_at	0.0294	0.00002133	1.23	Atp2a2	ATPase sarcoplasmic/endoplasmic reticulum Ca2+ transporting 2
1390432_at	0.0294	0.00002109	1.03	Tmco3	transmembrane and coiled-coil domains 3
1372989_at	0.027	0.00000843	-1.51	Zdhhc14	zinc finger, DHHC-type containing 14
1398304_at	0.0453	0.00004841	-1.71	Fzd2	frizzled class receptor 2
1368368_a_at	0.043	0.0000405	-2.04	Lsr	lipolysis stimulated lipoprotein receptor
1390176_at	0.027	0.00001019	-2.56	Fam84b	family with sequence similarity 84, member B

adj.*p*-value < 0.05, log(FC) >1 or < -1.5

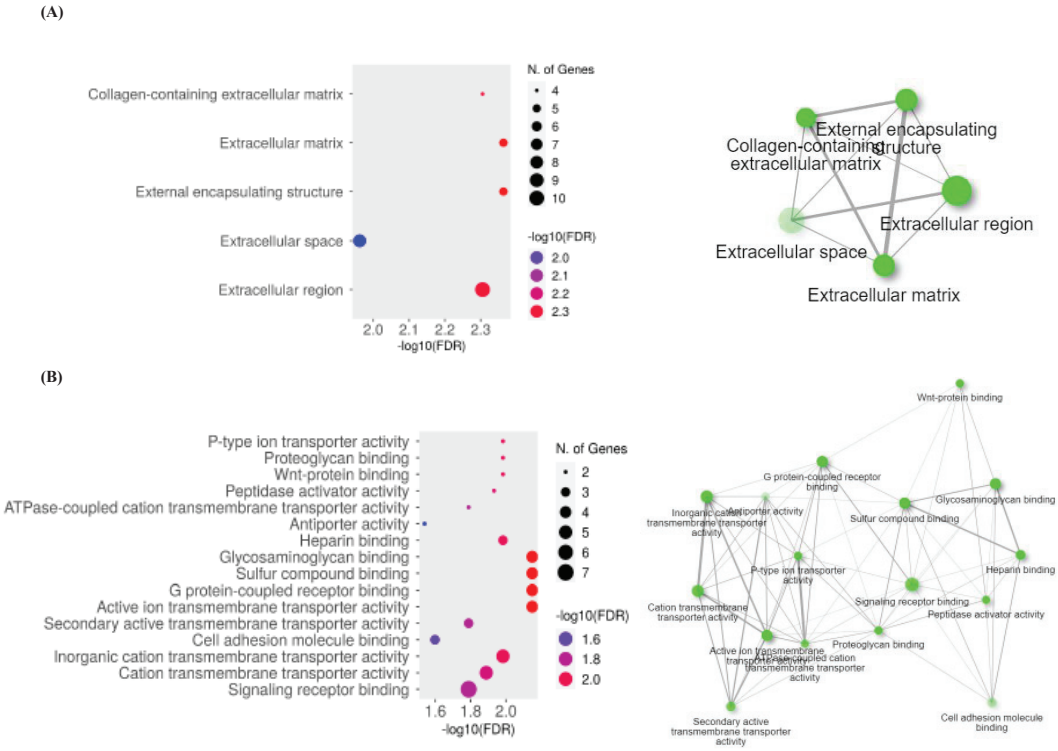

Figure 4 Analysis of 33 DEGs' functional enrichment. (A) cellular component and (B) molecular function GO enrichment of the DEGs. The number of genes is indicated by the size of the circles. There are more genes present when the circle is larger. Also included is the PPI network. FDR p-value cutoff = 0.05 and Edge cutoff = 0.2.

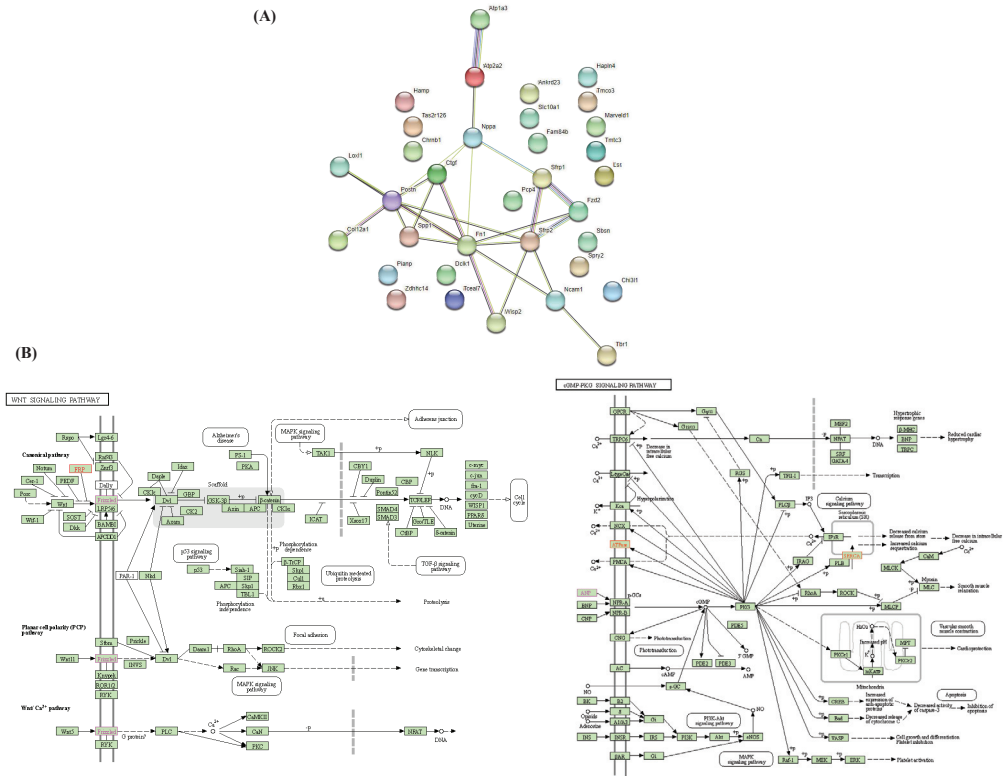

Figure 5 Identification of genes of interest. (A) PPI network analysis using STRING online tools and (B) pathway enrichment analysis of DEGs by KEGG using DAVID online tools.

Table 5: Significantly impacted signaling pathways in GSE47495 and GSE9694 data series.

Enrichment FDR	Pathway Genes	Fold Enrichment	Pathway	Genes
0.044	1583	14.08	Wnt signaling pathway	Sfrp2, Sfrp1, Fzd2
0.044	164	13.56	CGMP-PKG signaling pathway	Atp2a2, Atp1a3, Nppa

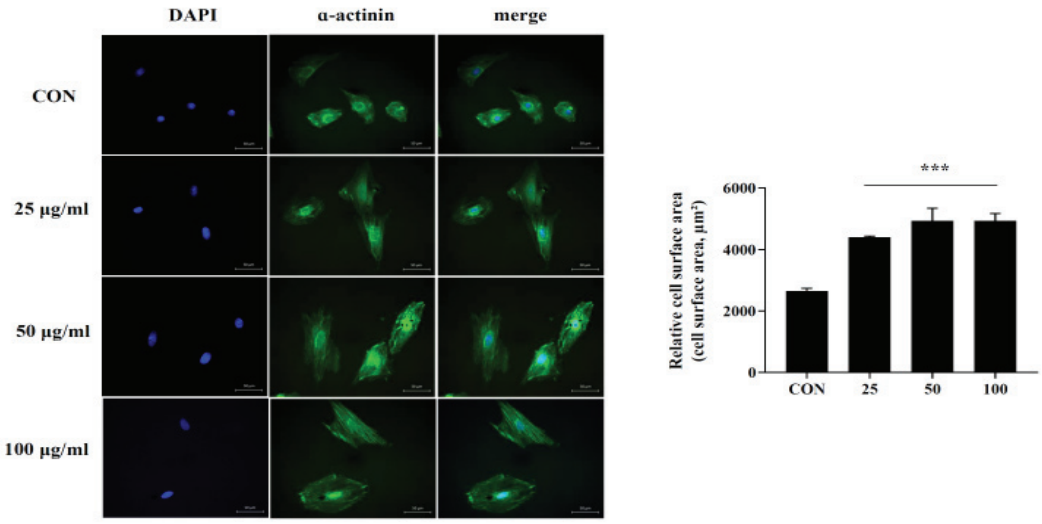

Figure 6 Cell surface area measurement in DPM-treated H9C2 cells. Representative images of H9C2 cells stained with anti-α-actinin antibody and DAPI (for the nucleus). Cell surface area was measured using ZEISS ZEN 3.7 software. Data are expressed as cell surface area ± SEM of triplicate samples. ***$p < 0.001$ vs. CON.

PPI network and KEGG analysis

As shown in figure 5A, we mapped the PPIs using STRING to distinguish connections among the 33 genes. The network is composed of 33 nodes and 26 edges, and has an average local clustering coefficient of 0.285. The STRING database was used to analyze the numerous proteins, and the results showed that two biological signaling pathways, the Wnt and CGMP-PKG signaling pathways, were considerably impacted. Using DAVID, KEGG analysis simultaneously showed that the DEGs in CGMP-PKG and Wnt signaling pathways were highly enriched (Figure 5B). The gene list shown in table 5.

Cell surface area measurement

Myocardial disease is a physiological response of the heart to external and internal stimuli. Various pathophysiological stimuli promote a complex remodeling process in the heart, accompanied by cardiomyocyte loss, existing cardiomyocytes cell size enlargement, and cardiac hypertrophy, leading to ischemic and hypertrophic phenotypes [18]. Therefore, we investigated whether DPM could induce myocardial hypertrophy *in vitro*. H9C2 cells were treated with different concentrations of DPM for 3h, followed by immunostaining with α-actinin to measure cell size, as previously described. Our results showed that the DPM treatment group had markedly increased cell size compared to that in the control group (Figure 6).

Validation of DEGs data using qRT-PCR

To verify the transcriptome data acquired after treating H9C2 cells with DPM for 24h, we used qRT-PCR using RNA extracted from stimulated cells. Among the analyzed transcripts, sfrp1, sfrp2, fzd2, and nppa showed similar expression profiles (Figure 7). DPM treatment appears to partially affect the Wnt-signaling pathway. The increased expression of fetal genes, such as natriuretic peptide precursor A (nppa) and natriuretic peptide precursor B (nppb), is associated with pathological hypertrophy [19,20]. We also investigated the expression levels of fetal gene mRNAs using qRT-PCR. There were significant increases in fetal gene expression at the transcriptional level, suggesting that there are mechanisms by which DPM facilitates myocardial hypertrophy (Figure 7).

Conclusion

We investigated the biological relationship

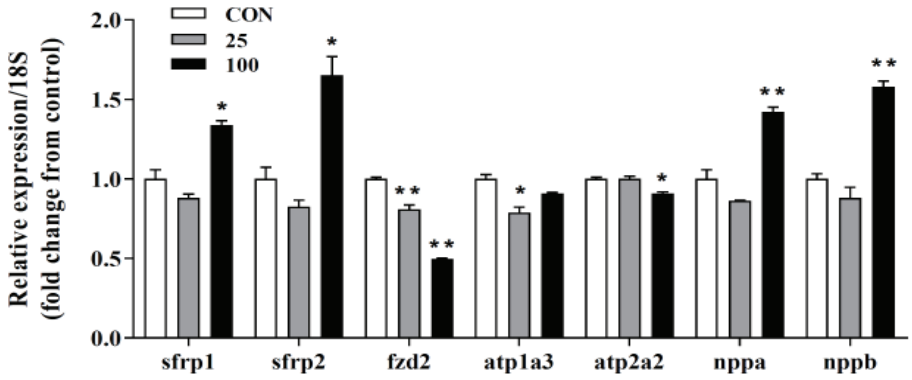

Figure 7 Hub gene expression levels in DPM-treated H9C2 cells. qRT-PCR was used to confirm the changes in hub gene expression after 24 h of DPM treatment in H9C2 cells. The results of three duplicate samples are expressed as fold changes by SEM. *p < 0.05, and **p < 0.01 vs. CON.

between DPM and myocardial infarction based on the GEO database and bioinformatics. A total of 33 differently expressed genes were identified and their possible signaling networks were investigated. Furthermore, we revealed the activation of two cellular signaling pathways. In addition to increasing the prediction accuracy, the use of experimental validation and literature-based analysis in our study aids in understanding the mechanisms underlying DPM-related cardiac hypertrophy. The study results will be useful as a basis for future in-depth investigations.

Acknowledgment

Author contribution

This version of the article has been read and approved by all authors.

Funding

Not applicable.

Conflict of interest

The authors declare no conflict of interest.

References

1. Giamouzis G, Dimos A, Xanthopoulos A, Skoularigis J, Triposkiadis F. Left ventricular hypertrophy and sudden cardiac death. Heart Fail Rev. 2022 Mar;27(2):711-724. doi: 10.1007/s10741-021-10134-5. Epub 2021 Jun 28. PMID: 34184173.
2. Kang YJ. Cardiac hypertrophy: a risk factor for QT-prolongation and cardiac sudden death. Toxicol Pathol. 2006;34(1):58-66. doi: 10.1080/01926230500419421. PMID: 16507545.
3. Shenasa M, Shenasa H. Hypertension, left ventricular hypertrophy, and sudden cardiac death. Int J Cardiol. 2017 Jun 15;237:60-63. doi: 10.1016/j.ijcard.2017.03.002. Epub 2017 Mar 3. PMID: 28285801.
4. Liu R, Molkentin JD. Regulation of cardiac hypertrophy and remodeling through the dual-specificity MAPK phosphatases (DUSPs). J Mol Cell Cardiol. 2016 Dec;101:44-49. doi: 10.1016/j.yjmcc.2016.08.018. Epub 2016 Aug 27. PMID: 27575022; PMCID: PMC5154921.
5. Zhang QJ, Tran TAT, Wang M, Ranek MJ, Kokkonen-Simon KM, Gao J, Luo X, Tan W, Kyrychenko V, Liao L, Xu J, Hill JA, Olson EN, Kass DA, Martinez ED, Liu ZP. Histone lysine dimethyl-demethylase KDM3A controls pathological cardiac hypertrophy and fibrosis. Nat Commun. 2018 Dec 7;9(1):5230. doi: 10.1038/s41467-018-07173-2. PMID: 30531796; PMCID: PMC6286331.
6. MacDonald MR, Petrie MC, Hawkins NM, Petrie JR, Fisher M, McKelvie R, Aguilar D, Krum H, McMurray JJ. Diabetes, left ventricular systolic dysfunction, and chronic heart failure. Eur Heart J. 2008 May;29(10):1224-40. doi: 10.1093/eurheartj/ehn156. Epub 2008 Apr 18. PMID: 18424786.
7. McEntee JC, Ogneva-Himmelberger Y. Diesel particulate matter, lung cancer, and asthma incidences along major traffic corridors in MA, USA: A GIS analysis. Health Place. 2008 Dec;14(4):817-28. doi: 10.1016/j.healthplace.2008.01.002. Epub 2008 Jan 11. PMID: 18280198..
8. Gamble J. Lung cancer and diesel exhaust: a critical review of the occupational epidemiology literature. Crit Rev Toxicol. 2010 Mar;40(3):189-244. doi: 10.3109/10408440903352818. PMID: 20156057.
9. Benbrahim-Tallaa L, Baan RA, Grosse Y, Lauby-Secretan B, El Ghissassi F, Bouvard V, Guha N, Loomis D, Straif K; International Agency for Research on Cancer Monograph Working Group. Carcinogenicity of diesel-engine and gasoline-engine exhausts and some nitroarenes. Lancet Oncol. 2012 Jul;13(7):663-4. doi: 10.1016/s1470-2045(12)70280-2. PMID: 22946126.
10. Yan YH, Chen TB, Yang CP, Tsai IJ, Yu HL, Wu YS, Huang WJ, Tseng ST, Peng TY, Chou EP. Long-term exposure to particulate matter was associated with increased dementia risk using both

traditional approaches and novel machine learning methods. Sci Rep. 2022 Oct 12;12(1):17130. doi: 10.1038/s41598-022-22100-8. PMID: 36224306; PMCID: PMC9556552.

11. Hamanaka RB, Mutlu GM. Particulate Matter Air Pollution: Effects on the Cardiovascular System. Front Endocrinol (Lausanne). 2018 Nov 16;9:680. doi: 10.3389/fendo.2018.00680. PMID: 30505291; PMCID: PMC6250783.

12. Du Y, Xu X, Chu M, Guo Y, Wang J. Air particulate matter and cardiovascular disease: the epidemiological, biomedical and clinical evidence. J Thorac Dis. 2016 Jan;8(1):E8-E19. doi: 10.3978/j.issn.2072-1439.2015.11.37. PMID: 26904258; PMCID: PMC4740122.

13. Costello S, Attfield MD, Lubin JH, Neophytou AM, Blair A, Brown DM, Stewart PA, Vermeulen R, Eisen EA, Silverman DT. Ischemic Heart Disease Mortality and Diesel Exhaust and Respirable Dust Exposure in the Diesel Exhaust in Miners Study. Am J Epidemiol. 2018 Dec 1;187(12):2623-2632. doi: 10.1093/aje/kwy182. PMID: 30137203; PMCID: PMC6269247.

14. Torén K, Bergdahl IA, Nilsson T, Järvholm B. Occupational exposure to particulate air pollution and mortality due to ischaemic heart disease and cerebrovascular disease. Occup Environ Med. 2007 Aug;64(8):515-9. doi: 10.1136/oem.2006.029488. Epub 2007 Feb 15. PMID: 17303673; PMCID: PMC2078490.

15. Zuo L, Youtz DJ, Wold LE. Particulate matter exposure exacerbates high glucose-induced cardiomyocyte dysfunction through ROS generation. PLoS One. 2011;6(8):e23116. doi: 10.1371/journal.pone.0023116. Epub 2011 Aug 5. PMID: 21850256; PMCID: PMC3151271..

16. Cao Y, Long J, Ji Y, Chen G, Shen Y, Gong Y, Li J. Foam cell formation by particulate matter (PM) exposure: a review. Inhal Toxicol. 2016 Nov;28(13):583-590. doi: 10.1080/08958378.2016.1236157. Epub 2016 Oct 6. PMID: 27706953.

17. Park JH, Nho KJ, Lee JY, Yoo YJ, Park WJ, Cho C, Kim DH. Anti-Ischemic Effects of PIK3IP1 Are Mediated through Its Interactions with the ETA-PI3Kγ-AKT Axis. Cells. 2022 Jul 11;11(14):2162. doi: 10.3390/cells11142162. PMID: 35883611; PMCID: PMC9322903.

18. Burchfield JS, Xie M, Hill JA. Pathological ventricular remodeling: mechanisms: part 1 of 2. Circulation. 2013 Jul 23;128(4):388-400. doi: 10.1161/CIRCULATIONAHA.113.001878. PMID: 23877061; PMCID: PMC3801217.

19. Izumo S, Nadal-Ginard B, Mahdavi V. Protooncogene induction and reprogramming of cardiac gene expression produced by pressure overload. Proc Natl Acad Sci U S A. 1988 Jan;85(2):339-43. doi: 10.1073/pnas.85.2.339. PMID: 2963328; PMCID: PMC279543.

20. Song HK, Hong SE, Kim T, Kim DH. Deep RNA sequencing reveals novel cardiac transcriptomic signatures for physiological and pathological hypertrophy. PLoS One. 2012;7(4):e35552. doi: 10.1371/journal.pone.0035552. Epub 2012 Apr 16. PMID: 22523601; PMCID: PMC3327670.

How to cite this article: Nho KJ, Shin JH. Bioinformatic Analysis of the Association Between Myocardial Disease and Diesel Particulate Matter. 2023 Apr 04; 4(4): 590-599. doi: 10.37871/jbres1714, Article ID: JBRES1714, Available at: https://www.jelsciences.com/articles/jbres1714.pdf